REGULAR ARTICLE

blood advances

Membrane curvature and PS localize coagulation proteins to filopodia and retraction fibers of endothelial cells

Christopher V. Carman,[1,2] Dessislava N. Nikova,[2] Yumiko Sakurai,[3,4] Jialan Shi,[2,5,6] Valerie A. Novakovic,[2] Jan T. Rasmussen,[7] Wilbur A. Lam,[3,4] and Gary E. Gilbert[2,5,6]

[1]Harvard School of Public Health, Boston, MA; [2]Department of Medicine, VA Boston Healthcare System, Boston, MA; [3]Wallace H. Coulter Department of Biomedical Engineering, Georgia Institute of Technology and Emory University, Atlanta, GA; [4]Aflac Cancer and Blood Disorders Center, Children's Healthcare of Atlanta and Emory University, Atlanta, GA; [5]Department of Medicine, Brigham and Women's Hospital, Boston, MA; [6]Department of Medicine, Harvard Medical School, Boston, MA; and [7]Protein Chemistry Laboratory, Department of Molecular Biology and Genetics, Aarhus University, Aarhus, Denmark

Key Points

- Convex membrane curvature and phosphatidylserine create discrete binding locations for lactadherin and coagulation factor V(a).
- Stressed endothelial cells extend filaments with both high convexity and PS, establishing discrete sites of prothrombinase activity.

Prior reports indicate that the convex membrane curvature of phosphatidylserine (PS)-containing vesicles enhances formation of binding sites for factor Va and lactadherin. Yet, the relationship of convex curvature to localization of these proteins on cells remains unknown. We developed a membrane topology model, using phospholipid bilayers supported by nano-etched silica substrates, to further explore the relationship between curvature and localization of coagulation proteins. Ridge convexity corresponded to maximal curvature of physiologic membranes (radii of 10 or 30 nm) and the troughs had a variable concave curvature. The benchmark PS probe lactadherin exhibited strong differential binding to the ridges, on membranes with 4% to 15% PS. Factor Va, with a PS-binding motif homologous to lactadherin, also bound selectively to the ridges. Bound factor Va supported coincident binding of factor Xa, localizing prothrombinase complexes to the ridges. Endothelial cells responded to prothrombotic stressors and stimuli (staurosporine, tumor necrosis factor-α [TNF- α]) by retracting cell margins and forming filaments and filopodia. These had a high positive curvature similar to supported membrane ridges and selectively bound lactadherin. Likewise, the retraction filaments and filopodia bound factor Va and supported assembly of prothrombinase, whereas the cell body did not. The perfusion of plasma over TNF-α–stimulated endothelia in culture dishes and engineered 3-dimensional microvessels led to fibrin deposition at cell margins, inhibited by lactadherin, without clotting of bulk plasma. Our results indicate that stressed or stimulated endothelial cells support prothrombinase activity localized to convex topological features at cell margins. These findings may relate to perivascular fibrin deposition in sepsis and inflammation.

Introduction

Quiescent cells maintain phosphatidylserine (PS) on the inner leaflet of the plasma membrane and do not display PS-containing binding sites for factor V(a) or support prothrombinase activity. After stimulation and very early in apoptosis, cells expose limited quantities of PS on discrete regions of the

Submitted 17 December 2021; accepted 29 June 2022; prepublished online on *Blood Advances* First Edition 18 July 2022; final version published online 29 December 2022. https://doi.org/10.1182/bloodadvances.2021006870.

Primary data sets will be shared upon request in compliance with the policies of *Blood Advances* and the National Institutes of Health (NIH) and the Department of Veterans Affairs to gary.e.gilbert.md@gmail.com.

The full-text version of this article contains a data supplement.

plasma membrane.[1-4] This PS exposure is frequently below the threshold that supports binding of the PS probe annexin A5, and PS exposure is frequently reversible.[5-7] However, in vivo data imply that this limited, localized PS exposure supports procoagulant function. For example, staining of injured vessels during intravital thrombus formation have not reliably found PS-rich, annexin A5 binding, apoptotic cells, or microparticles that colocalize with fibrin deposition.[8,9]

We have shown in other studies that lactadherin and annexin A5 differentially bind discrete PS-containing membrane sites on multiple cell types, including platelets, leukemia cells, and red blood cells.[1-3,8,10,11] Moreover, lactadherin and annexin A5 exhibit differential abilities to functionally block exposed procoagulant surface PS.[1-3,8,11-14] These findings imply the value of lactadherin and annexin A5 as probes that may help to illuminate focal PS exposure on cell membranes but do not clarify the properties that enable lactadherin and annexin A5 to preferentially bind disparate sites.

Lactadherin exhibits stereospecific binding to phosphatidyl-L-serine and a strong preference for highly convex vesicle membranes.[15,16] Binding is mediated by both hydrophobic spikes that partially penetrate the membrane and charged residues that form salt bridges, particularly with anionic moieties of PS. It has been used as a probe for exposed PS and as an inhibitor of PS-dependent procoagulant activity.[1-3,8,13] Annexin A5 is representative of another type of PS-binding proteins and is also frequently used as a probe for PS exposure on apoptotic cells.[17-21] Annexin A5 binds membranes through, Ca^{++}-dependent, ionic interactions with no penetration of the membrane. Annexin A5 requires a higher membrane PS content than lactadherin, and binding is cooperative, with annexin A5 forming trimers on the membrane surface.[22] Annexin A5 exhibits a lower degree of specificity for phosphatidyl-L-serine vs other negatively charged lipids and prefers membranes that are flat or have concave curvature.[22] Indeed, clusters of membrane-bound annexin A5 can induce regions of concave curvature in a cell membrane.[23] In this study, we explored the relationship between membrane curvature and binding of lactadherin and annexin A5 on both synthetic membranes and cells.

Factor V is a 330-kDa glycoprotein that circulates in plasma.[24] Upon encountering a PS-containing membrane and after proteolytic activation, it serves as a membrane-bound cofactor for factor Xa.[25] The membrane-bound factor Va-factor Xa complex (prothrombinase complex) efficiently cleaves prothrombin to thrombin in the common coagulation pathway. The membrane-binding C domains of factor V(a) share sequence homology with lactadherin and bind membranes in a similar manner.[26-28] Factor V(a) recognizes membrane phosphatidyl-L-serine in a stereospecific manner[29] and has a strong preference for highly convex phospholipid vesicles.[13,30] Surprisingly, the relationship of convex membrane curvature to localization and function of the prothrombinase complex on cell membranes remains largely unexplored.

Quiescent endothelia form a blood barrier that is anticoagulant.[31-34] However, in response to cellular stress or stimulation, they undergo several changes that confer limited procoagulant properties.[35,36] In particular, the cell margins topologically rearrange into thin (20-100 nm) filaments and filopodia and partially retract, exposing the subendothelial matrix at intercellular gaps.[37-43] Recent data also indicate that endothelial cells expose PS in response to a variety of stimuli, even in the absence of apoptosis.[44-48] Moreover, several studies have either implicated or directly demonstrated that the prothrombinase complex can assemble on endothelial surfaces.[36,48,49] These observations motivated us to explore the relationship between membrane convexity on the filaments and filopodia and binding sites for factor V on stressed and stimulated endothelial cells.

In this study, we used a novel technique to compare binding of lactadherin and annexin A5 to convex and concave membrane regions on the same synthetic membrane. We compared binding of factor Va and assembly of the prothrombinase complex to lactadherin and annexin A5. We then hypothesized that the location of binding sites for factor V(a) and the assembly of the prothrombinase complex would be on highly convex fibrils and filopodia and correlate with the location of binding sites for lactadherin on stressed or stimulated endothelial cells. Indeed, we found that the prothrombinase complex assembled preferentially on convex portions of supported membranes as well as convex filopodia and membrane filaments of endothelial cells. The localized prothrombinase complex was functional, leading to thrombin generation and to localized fibrin deposition. The results indicate that membrane topology influences the location of prothrombinase complex assembly on endothelial cells.

Materials and methods

For antibodies and reagents, labeling proteins, phospholipid vesicles, cell culture and stimulation, prothrombinase activity, and lactadherin competition see the supplemental Materials.

Fabricated silica substrates and supported bilayers

We designed silica substrates to confer a defined positive membrane curvature.[50-52] Silica wafers were prepared to our specifications by Team Nanotec GmbH (Villingen-Schwenningen, Germany). Substrates were etched as an array of parallel ridges with interridge spacing of 7.5 μm within a 3 × 6-mm rectangle on a 7 × 7-mm substrate. The convex radii of curvature on the ridges were either +10 nm or +30 nm, mimicking the curvature of sonicated phospholipid vesicles and filopodia.[53] Troughs had concave curvature of approximately −300 nm, with variably-spaced etched ridges, confirmed by scanning electron microscopy. The silica substrates were cleaned by immersing for 30 minutes in sulfuric acid/hydrogen peroxide (3:1 v/v), rinsed with Tris-buffered saline, then in filtered deionized water. The lipid bilayer was deposited by incubating a 200-μL suspension of small unilamellar vesicles on the substrate in dark for 1 hour at 22°C. Residual vesicles were removed by gently rinsing with phosphate-buffered saline (PBS). The supported bilayers were maintained in PBS at 22°C and used within 6 hours. The phospholipid vesicles contained PS, L-α-phosphatidylethanolamine (PE), and phosphatidylcholine (PC) at ratios of 0:20:80; 4:20:76, 10:20:70, and 15:20:65. In some cases, the PE fraction was spiked with rhodamine-PE (PE:Rhod-PE, 19.5:0.5).

Supported bilayers were incubated with the indicated fluorescent proteins (10 nM lactadherin, annexin A5, factor Va, or factor Xa) for 15 minutes in the dark at 22°C. The bilayers were then rinsed with Tris-buffered saline+Ca^{2+} and imaged immediately by confocal microscopy. To maintain the bilayers/substrates in stable aqueous suspension during imaging, we implemented a custom-designed sample holder composed of a microscope glass, a silicon O-ring spacer, and a coverslip.

Atomic force and confocal microscopy

Atomic force microscopy (AFM) was conducted within a vibration/acoustic isolation hood using an ESPM 3D atomic force microscope, equipped with a sample holder for measurements in liquid (Novascan Technologies, Inc, Ames, IA) integrated with a C1si Confocal Microscope System (Nikon Instruments Inc, Melville, NY). For contact mode AFM scanning, we used MLCT Silicon Nitride Probes with a cantilever spring constant of 0.07 N/m (Veeco Probes Inc, Plainview, NY). For tapping mode scanning, we used NSC Silicon Probes with a cantilever spring constant of 5.0 N/m (Mikromasch; San Jose, CA) at a scan rate of 0.5 Hz. Optical imaging was performed at 22°C in the dark using CFI Plan APO DM 60× and 100× oil-immersion objectives (Nikon Instruments Inc) using 488-, 561-, and 639-nm laser excitation wavelengths. Data were processed with EZ-C1 image processing software (Nikon Instruments Inc, Melville, NY). Additional optical imaging was performed with the Confocal Laser Scanning Microcopy system LSM 710/ConfoCor3 (Carl Zeiss MicroImaging, LLC, Jena, Germany) equipped with an Ar laser (488 nm), a DPSS laser (561 nm), and an HeNe laser (633 nm) using IC^2S Plan APO 40× and 64× oil-immersion objectives. Data acquisition and analysis were performed in ZEN software (Carl Zeiss MicroImaging, LLC).

Fibrin deposition on endothelium

Human umbilical endothelial cells (HUVECs) were grown on standard culture plates and treated with 100 ng/mL tumor necrosis factor-α (TNF-α) for 4 hours. The cells were then overlaid with fresh recalcified plasma, partially anticoagulated with corn trypsin inhibitor and 0.1 IU/mL heparin (equivalent to the concentration used to treat thromboembolism), and maintained with continuous gentle mixing at 37°C in a 5% CO_2 cell culture incubator. after 15, 30, or 60 minutes, individual plates were withdrawn, rinsed, fixed, and stained with FITC-59D8 against fibrin and 4′,6-diamidino-2-phenylindole (nuclear stain). Imaging was performed with confocal fluorescence and differential interference contrast microscopy.[54]

Fibrin deposition on endothelium in engineered microvessels under flow

Engineered microvessel arrays lined with confluent HUVECs were prepared as described[55] and pretreated with 100 ng/mL TNF-α overnight, for plasma experiments, or 50 ng/mL for 4 hours for whole-blood experiments. Vessel microarrays were then perfused with fresh plasma treated with corn trypsin inhibitor, supplemented with fluorescein-labeled fibrinogen, at shear rates of 10 to 500 seconds^{-1}. In some studies, the plasma membrane of the HUVECs was concomitantly labeled by co-perfusion with CellMask Orange or Deep Red, per the manufacturer's specifications (Invitrogen). Subsequently, the microvessels were rinsed with PBS and fixed with 3.7% formaldehyde. In some cases, the samples were subsequently stained with anti-VE-cadherin-FITC antibody (1:200 dilution; Cell Signaling) to mark the adherens junctions. Imaging was conducted with an Axio Observer LSM 700 (Carl Zeiss) laser scanning confocal microscope.

Results

We hypothesized that convex ridges would provide topological motifs capable of localizing coagulation-related proteins. Accordingly, we fabricated silica substrates with a defined positive curvature to support lipid bilayers. The ridges of the substrate have radii of +10 or +30 nm, alternating with concave troughs with radii of approximately −300 nm (Figure 1A-B). The silica surfaces were used to support fusion of suspended lipid vesicles to form lipid bilayers conforming to the silica substrate.[56] The bilayers were composed of PS (0%, 4%, 10%, or 15%) and PE (20%), with the balance made up of PC. To visualize the supported bilayers we

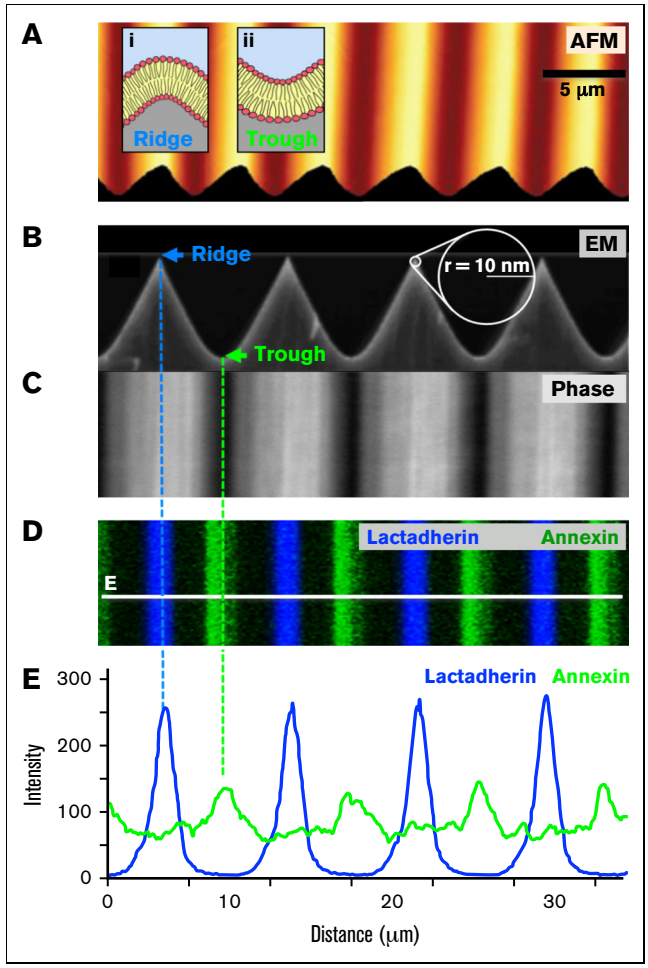

Figure 1. Lactadherin binds convex ridges of supported membranes and annexin A5 binds concave valleys. We fabricated chemically etched silica nanoridge/-trough substrates as described in "Materials and methods." (A) Color-coded AFM topographic image of a representative substrate containing ridges (yellow) and troughs (orange/brown) with radii of curvature of +10 and −300 nm, respectively. Insets i and ii: schematics of the expected positively and negatively curved lipid bilayers formed on the ridges and troughs, respectively. (B) A high-resolution scanning electron microscopy side-view image of the substrate. (C) Top-down phase images of the substrate showing brightly reflective ridges and dark troughs. (D) Substrates were overlaid with lipid bilayers containing 4% PS, 20% PE, and 76% PC followed by incubation with 10 nM lactadherin-alexa-647 (blue pseudocolor) and 10 nM annexin A5-FITC (green) in the presence of calcium and imaged by serial-section confocal microscopy. Compressed z stacks are represented as a maximum-intensity projection image. (E) Fluorescence intensity profiles corresponding to the white line in panel D. Lactadherin preferentially bound to the positively curved ridges, whereas annexin A5 selectively bound to the negatively curved troughs (dashed lines). Additional quantitative evaluation displayed in supplemental Figure 1.

spiked the PE fraction with 0.5% fluorescent rhodamine-PE. Through confocal microscopy (supplemental Figure 1A) and fluorescence recovery after photobleaching (not shown), we confirmed that lipids of these bilayers covered the silica substrate and retained the expected lateral mobility of the lipids.

Supported bilayers containing 4% PS were incubated with fluorescence-labeled lactadherin and annexin A5 and imaged with confocal fluorescence microscopy (Figure 1). In phase contrast the ridges appeared bright, troughs dark (Figure 1C) Lactadherin exhibited a preference for positively curved ridges, whereas annexin A5 preferred flat and negatively curved troughs (Figure 1D-E). The fluorescence intensity ratio was at 16:1 ridge/trough for lactadherin. Fluorescence intensity ratio for annexin was lower at 1:2 ridge/trough for annexin A5. However, the fluorescence ratio may not precisely reflect the quantity of protein bound or the exact distribution that either protein would have in the absence of the other (supplemental Figure 2A). In fact, we found that annexin A5 and lactadherin binding was more evenly distributed in the absence of the other. Only lactadherin exhibited enhanced binding on the convex ridges (supplemental Figure 1B). Thus, co-staining of the ridges enhances the preference of each protein for differing curvatures. We found similar topological preferences for lactadherin and annexin A5 on membranes with 10% or 15% PS, indicating a similar relevance for curvature over a range of physiologic PS content. Neither lactadherin nor annexin A5 bound detectably to PC/PE bilayers lacking PS, indicating that curvature alone was insufficient to form binding sites (supplemental Figure 2A). Lactadherin bound in the same manner in the absence of calcium, whereas annexin A5 binding was not observed (supplemental Figure 2B), confirming the known dependence of annexin A5 binding on calcium.[15,19,21,57-59] These results indicate that membrane curvature can substantially influence the location of these proteins.

We treated HUVECs with staurosporine to determine whether the preapoptotic pattern of lactadherin and annexin A5 binding is comparable to that previously observed on HELA cells.[2] Staurosporine-treated HUVECs retracted from neighboring cells, developing retraction filaments and filopodia-like protrusions as well as binding sites for both lactadherin and annexin A5 (Figure 2B). Lactadherin bound to subsets of retraction/filopodial structures at the cell margins (Figure 2C). In addition, the cell body contained distinct, nonoverlapping punctate binding sites for either lactadherin or annexin A5 (Figure 2D). Control HUVECs remained spread and supported little lactadherin or annexin A5 binding (Figure 2A). The dependence of lactadherin binding on exposed PS, rather than activated integrins, was confirmed by demonstrating complete blocking of lactadherin binding with an anti C2 domain antibody[8] (not shown).

Treatment with TNF-α, a prothrombotic and proinflammatory stimulus for HUVECs,[35,42,43,60] produced a contractile response similar to the early staurosporine response. The cells formed thin marginal structures comparable to those seen with staurosporine treatment (supplemental Figure 3C-E). These showed a mixture of phenotypes including both gap-associated retractile filaments (supplemental Figure 3D) and gap-absent filopodial protrusions at intact junctions (supplemental Figure 3E). TNF-α also induced formation of distinct lactadherin binding sites on marginal retraction filaments and filopodia (supplemental Figure 4B), as well as on cell body puncta (supplemental Figure 4C). These were distinct from annexin A5 punctate binding sites (not shown).

To further investigate the topological features of the lactadherin binding sites, we imaged using the scanning AFM fluid phase in tapping mode to minimally perturb the living cells. The cell peripheries exhibited readily identifiable retraction filaments and filopodia (Figure 3A) that were similar to those in Figure 2C and supplemental Figure 3. These had heights that predicted radii of +20 to 30 nm, similar to the supported bilayers (Figure 3B-C). We performed sequential confocal fluorescence imaging followed by scanning AFM of the same field (Figure 3D-G). Cells remained viable and filopodia moved slightly with some shift in filopodia alignment between the fluorescence (Figure 3E) and AFM images (Figure 3F). We confirmed that the filopodial structures that supported lactadherin binding also had radii in the range of +20 to 30 nm (Figure 3G). These results are consistent with our findings with supported bilayers (Figure 1; supplemental Figure 1) and show that stressed endothelial cells localize lactadherin sites on membrane features with a high positive curvature.

Lactadherin and factor Va membrane-binding C domains share structural homology and a similar preference for binding sites on membranes with convex curvature.[26,28] Accordingly, we asked whether factor Va would preferentially bind convex ridges, leading to localized assembly of the prothrombinase complex. Because factor Va serves as the membrane-bound anchor for factor Xa in the prothrombinase complex, we assessed binding of both fluorescent factors Va and Xa to supported bilayers (Figure 4). Factor Va alone bound selectively to ridges with a ridge/valley ratio comparable to that of lactadherin (not shown). In contrast, binding of factor Xa alone was not detected at this concentration. When both proteins were incubated with the substrate they exhibited coincident binding to the convex ridges (Figure 4). Binding to ridges was similar on bilayers containing 4% and 15% PS, whereas neither protein bound to membranes lacking PS (not shown). This demonstrated that the prothrombinase complex localizes to convex membrane features with PS (Figure 4).

Next, we asked whether factor Va would bind to highly convex structures of endothelial cells, similar to lactadherin. Concomitant binding of fluorescent lactadherin and factor Va demonstrated that these molecules have highly overlapping distributions on filopodia, marginal filaments, and punctate sites on TNF-α–treated HUVECs (supplemental Figure 4). Binding of factors Va and Xa was virtually absent from quiescent HUVECs (Figure 5A-B). Filamentous projections connecting cells did not stain (5B arrow). However, after TNF-α treatment, HUVECs supported binding of factors Va and Xa to discrete marginal filaments and filopodia (Figure 5C-D) and punctate (Figure 5E-F) domains resembling the distribution of sites for lactadherin (Figure 2). As with supported bilayers, factor Xa binding was dependent on the presence of factor Va (not shown).

To verify that prothrombinase complex binding features on endothelial cells are comparable to the features rich with lactadherin binding sites, we measured inhibition of the prothrombinase complex by competing lactadherin. TNF-α pretreatment induced an approximately eightfold increase in HUVEC-supported prothrombinase activity, compared with untreated control cells (not shown). Addition of lactadherin led to dose-dependent inhibition with 50% and >90% inhibition at concentrations of 100 and 260 nM, respectively (Figure 5G). By contrast, inhibition by annexin A5 was less effective. Thus, the majority of functional prothrombinase activity on activated endothelial cells is supported by PS-containing

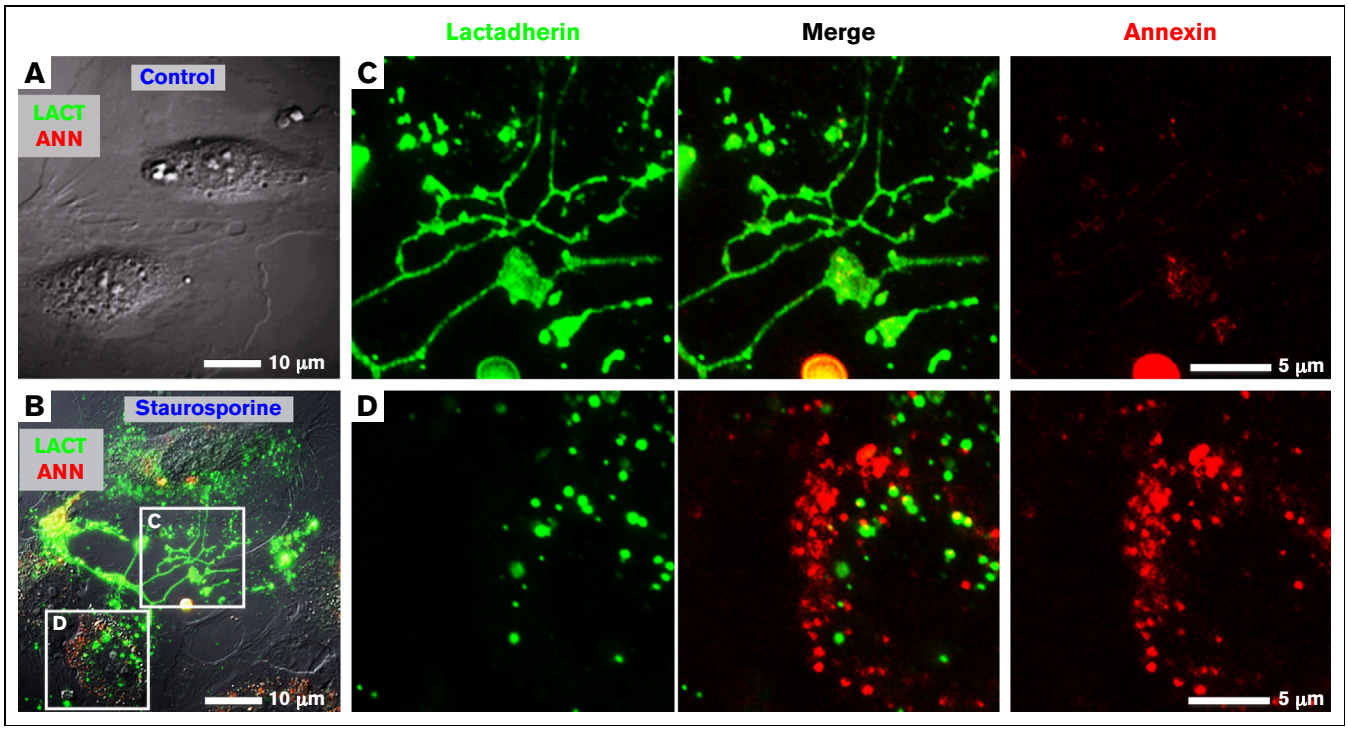

Figure 2. PS-containing features on staurosporine-treated HUVECs bind lactadherin or annexin A5. Staurosporine-treated HUVECs were incubated with 10 nM lactadherin-488 (green) and annexin A5-Cy3 (red) and visualized with live-cell imaging. (A) Representative image of control, vehicle-treated HUVECs with differential interference contrast (gray scale) and fluorescence lactadherin (green) and annexin A5 (red) overlaid. Note the absence of either green or red fluorescence. (B) HUVECs pretreated for 15 minutes with 0.5 μM staurosporine before incubation with lactadherin and annexin A5. The representative image shows strong binding of lactadherin and annexin A5 to submicrometer scale structures with filopodialike (C) and punctate (D) structures. (C-D) Enlarged views of boxed regions in panel B showing individual and merged fluorescence signals.

membrane sites that overlap with lactadherin binding sites, concentrated on convex cell features.

We hypothesized that focal procoagulant activity of stimulated or stressed endothelial cells on marginal filaments and filopodia would cause focal fibrin deposition near these structures. Presumably, the intact anticoagulant activity on the cell bodies would prevent clotting of bulk plasma. To test this hypothesis, we prepared subconfluent HUVEC monolayers and overlayed the cells with recalcified plasma, partially anticoagulated by 0.1 IU/mL heparin (equivalent to the concentration used as treatment for thromboembolism). After the indicated intervals, plates were fixed, and fibrin derived from native fibrinogen was imaged with fluorescein-labeled monoclonal antibody 59D8 (supplemental Figure 5A).[61] No fibrin accumulated on untreated control HUVECs after 60 minutes (supplemental Figure 5B). However, on TNF-α–treated HUVECs, focal fibrin deposits were readily evident at the cell margins by 15 minutes, with increased densities at 30 and 60 minutes (supplemental Figure 5B-D). Bulk plasma did not clot for up to 6 hours under these conditions (not shown). Fibrin deposition was highly attenuated by the addition of tissue factor pathway inhibitor or an anti-tissue factor antibody, indicating that the extrinsic pathway drives the focal fibrin formation (not shown). Thus, our data identified a tissue factor–mediated pathway through which TNF-α–treated endothelial cells mediated focal fibrin deposition.

We asked whether cultured endothelial cells would also support focal fibrin deposition in three-dimensional engineered microvessels exposed to plasma under physiologic shear force.[55] Thus, we used standard lithographic techniques to fabricate polydiethylsiloxane microchannels with dimensions comparable to postcapillary venules.[55] These were seeded with HUVECs, cultured to confluence and treated with TNF-α (Figure 6A). We next perfused these model microvessels with fresh plasma at a sheer of 500 seconds^{-1}, similar to microvasculature in vivo. To visualize the endothelial cell membranes and in situ fibrin deposition, we supplemented the perfusate with CellMask Deep Red (blue) and fluorescein-labeled fibrinogen (green), respectively. Consistent with our findings in supplemental Figure 5, no fibrin was deposited in the absence of TNF-α treatment (Figure 6B). However, in TNF-α–treated microvessels, significant fibrin deposition was evident within 30 minutes of perfusion. Fibrin concentrations marked cell-cell junctions (Figure 6C) indicating focal accumulation as predicted. Addition of lactadherin prevented fibrin accumulation, confirming that the process is dependent on exposed PS (Figure 6B; supplemental Figure 6).

We further asked whether intercellular junctions would remain the predominant location for fibrin accumulation when engineered microvessels were perfused with fresh whole blood (Figure 6D-H). Under these conditions, fibrin strands of varying thickness were visible, primarily aligned with the direction of fluid shear. Indeed, close examination revealed that the majority of fibrin strand initiation sites are discretely localized to the cell margins (Figure 6E, cyan arrows). In addition, most HUVEC boundaries are highlighted by a line of fibrin (Figure 6E-H). These were present both at intact and

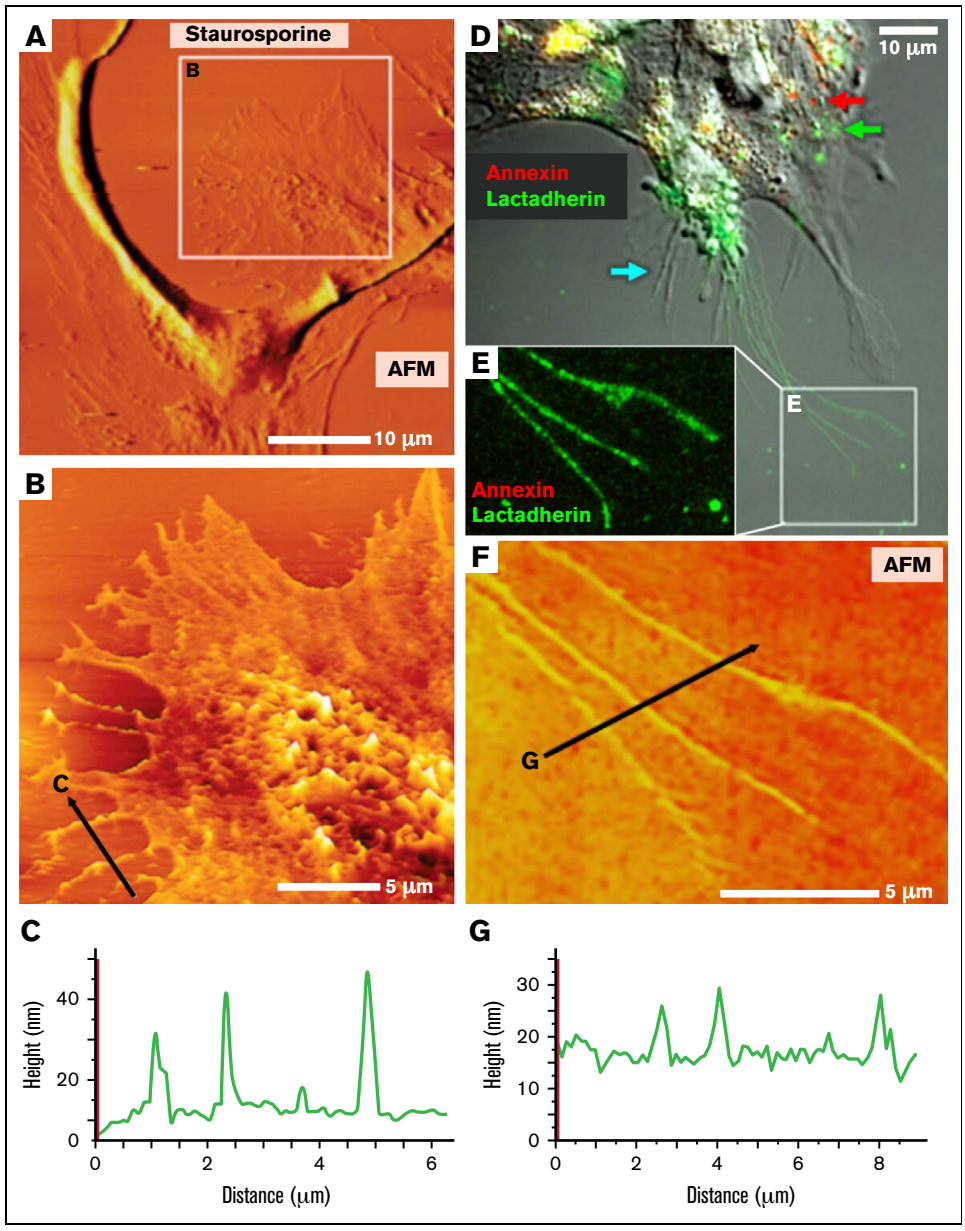

Figure 3. AFM topographic and fluorescence imaging of PS-containing domains on stressed HUVECs. (A) HUVECs grown on glass substrates and treated with staurosporine as in Figure 2 (0.5 μM, 15 minutes) followed by topographic AFM imaging, as described in "Materials and methods." The representative micrograph shows a cell undergoing retraction with filopodialike protrusions. (B) High-resolution scan of the boxed region in panel A. (C) Topographic profile of the retracted portion of the cell along the black line in panel B indicating that the heights of 3 individual filopodialike structures varied between ~20 and 30 nm. (D) HUVECs were treated with staurosporine, then incubated live with 10 nM lactadherin-488 (green) and annexin A5-Cy3 (red) and imaged by confocal and differential interference contrast (grayscale) microscopy. A representative image shows that the cell body contained punctate structures that preferentially bound either lactadherin or annexin A5 (eg, green and red arrows), though some areas of apparently coincident (yellow) binding were also noted. Thin filopodialike structures were at the periphery and a subset strongly bound lactadherin, but not annexin A5 (see box in panel E). Some filopodia bound neither lactadherin nor annexin A5 (cyan arrow). (E) A higher magnification fluorescent image of the area indicated in panel D. (F) High resolution AFM topographical scanning image of the cells protrusions shown by fluorescence in panel E. (G) Topographic profile of the protrusions along the line indicated in panel F, with a mean diameter of ~15 nm.

gap-containing junctions in which retraction filaments and filopodial protrusions were evident to varying degrees (Figure 6E-H; cyan and yellow arrows). Similar findings were made in experiments in which the junctions were visualized by staining of the specific marker VE-cadherin (supplemental Figure 7). Together, these findings support a model in which focal endothelia-supported procoagulant activity arises on highly curved filopodia and connecting filaments at the interface between stimulated cells.

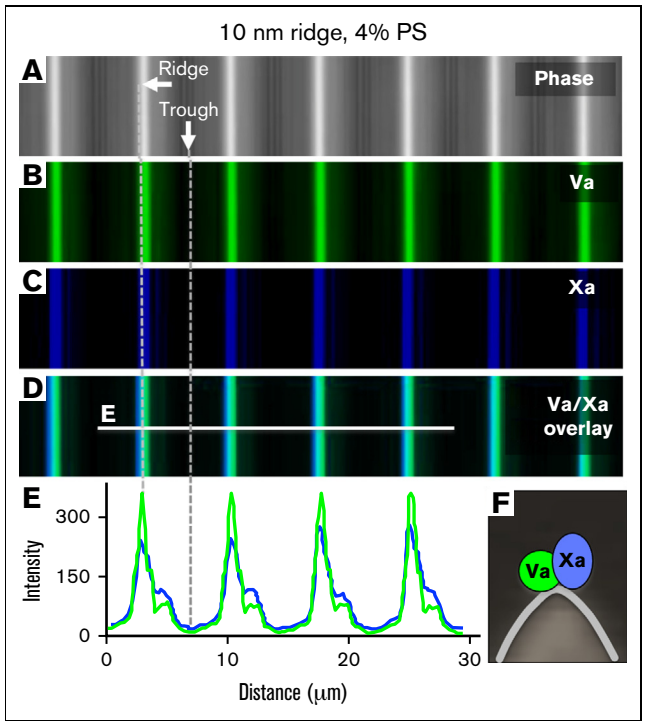

Figure 4. Factor Va binding sites and prothrombinase assembly localize to convex membrane ridges. Lipid bilayers containing 4% PS, 20% PE, and 76% PC were prepared on substrates with 10-nm radii ridges. Factor Va-Alexa 488, 10 nM (green) and 10 nM factor Xa-Alexa 647 (factor Xa-Glu-Gly-Arg-biotin/streptavidin-Alexa 647; blue) were incubated in the buffer overlaying the membrane ridges. (A) Differential interference contrast imaging mode localizes ridges (white) and troughs (dark) of the silica substrate. (B-C) Fluorescence images of bound factor Va–Alexa 488 and factor Xa–Alexa 647, respectively. (D) Overlay of images in panels A to C. (E) Fluorescence intensity line scans of the line in panel D shows that factors Va and Xa exhibited coincident and preferential binding to the convex ridges. See scheme in panel F.

Discussion

Our studies identify a mechanism for concentrating PS-binding proteins on topological features of the external plasma membrane. We show that topology can govern the binding and dominant location of lactadherin and annexin A5, leading to localization of factor Va and prothrombinase activity to filopodia and retraction filaments. The consequence of this localization is focal generation of thrombin and fibrin, leading to deposition of fibrin at intercellular junctions of stimulated endothelial cells.

Our results agree with prior observations indicating that lactadherin exhibits preference for PS-containing membranes with convex curvature.[15] Others have shown that annexin A5 binds preferentially to flat or concave surfaces.[22,62] In addition, we have shown that lactadherin and annexin A5 bind to discrete PS-containing membrane sites on stimulated or stressed platelets, leukemia cells, and HELA cells.[1-3,8,11,12] Lactadherin binding to HELA cells was largely restricted to filopodia and retraction fibers, similar to endothelial binding in this report. In this study, we used model membranes, supported by silica substrates with defined ridge curvature, to demonstrate that convex curvature of filopodia and other convex structures is an adequate mechanism for localizing binding of lactadherin and factor Va.

Prior studies report that activated endothelial cells bind factors Va and Xa, supporting prothrombinase complex activity.[48,49,63-66] Intravital imaging after laser-induced vessel injury showed that factor Va, factor Xa, prothrombinase, and fibrin all rapidly deposit on endothelial surfaces.[65,67-69] Our studies add to this body of information, using a less severe form of endothelial stress or stimulation. Under these conditions, the location of procoagulant activity is restricted in relation to more limited PS exposure and the topology of filopodia and retraction filaments at intercellular junctions.

Localization of enzymes and binding proteins in relation to membrane curvature is not novel. However, it has been primarily studied in the context of intracellular membranes. Curvature affects the localization of proteins that mediate vesicular trafficking as well as signaling via proteins, such as Arf-GAP1, dynamin, protein kinase C and phospholipase A2.[70-73] This study indicates that functional compartments linked to membrane convexity are also present on the exterior of cells.

We report use of membranes supported by engineered silica substrates as a new tool to visualize topology-dependent localization of membrane-binding proteins. We were able to verify the topographical preference of lactadherin and factor Va that had previously been reported. We anticipate further use of this methodology for the study of blood coagulation proteins, fibrinolytic proteins, and their inhibitors. In addition, we suggest that this methodology may find use in study of topological localization of proteins involved in cell fusion, vesicle fusion, and phagocytosis of apoptotic cells.

We hypothesize that the preference for curved membranes exhibited by lactadherin is related to its membrane binding mechanism. This involves insertion of amphipathic amino acid side chains, on surface-exposed spikes of the C2 domain, into the phospholipid membrane[28] Penetration is most likely enhanced by the decreased lateral pressure on convex membrane regions.[74] Notably, the C2 domain of factor V shares structural and sequence homology with that of lactadherin including conservation of amphipathic residues on exposed surface spikes.[27,28,75] In addition to PS, phosphatidylethanolamine enhances PS-mediated membrane binding of factor V,[76] but has little effect on lactadherin.[15] Phosphatidylethanolamine has direct interactions with factor V and also enhances PS-dependent membrane binding of vitamin K–dependent coagulation proteins such as factor Xa,[77] probably through the same mechanism. By contrast with lactadherin, the membrane-binding facet of annexin V is hydrophilic and nearly flat[57] and the mechanism appears related to Ca^{++}-mediated bridging of phosphate lipid moieties with a Ca^{++}-binding motif of annexin A5. Both PS and phosphatidylethanolamine also support binding of annexin A5 where binding can induce local concave curvature.[23]

The proposed membrane-binding mechanisms in the prior paragraph are readily reconciled with competitive membrane binding between lactadherin or annexin A5 and proteins of the prothrombinase complex. Lactadherin competes for factor V(a)–binding sites on synthetic membranes, whereas annexin A5 does not.[13] However, both lactadherin and annexin A5 can inhibit the prothrombinase complex, albeit with differing degrees of efficiency. Inhibition by annexin A5 occurs, presumably, through competition for binding of factor Xa and/or prothrombin; it increases with membrane PS and PE content and decreases with convexity.[13] We rationalize the partial inhibition of prothrombinase by annexin A5 on endothelial cells (Figure 5G) to indicate incomplete compartmentalization of

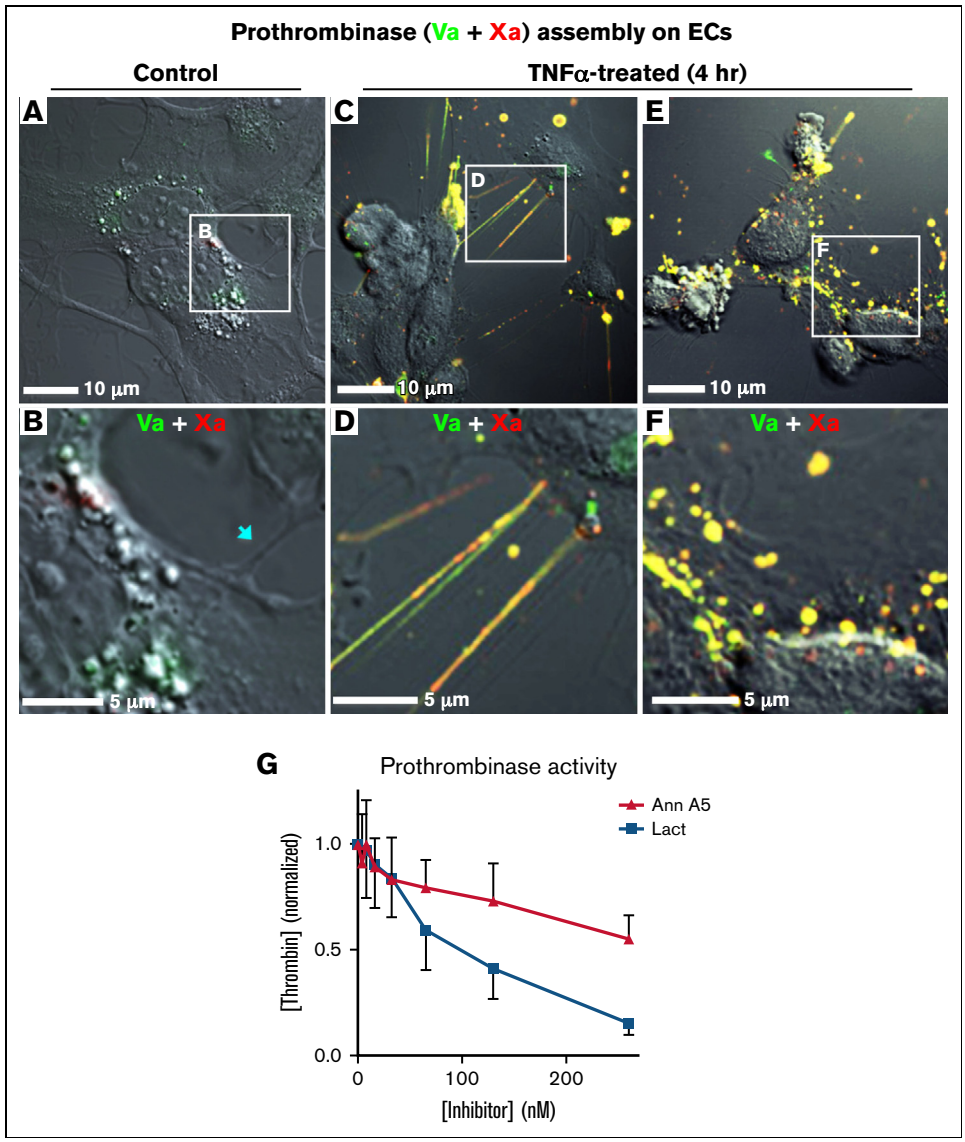

Figure 5. Topology-related assembly of prothrombinase complexes on TNF-α–activated HUVECs. Subconfluent HUVECs were treated with TNF-α (50 ng/mL, 4 hours) and then incubated with factor Va-Alexa 488, 10 nM (green) and 10 nM factor Xa-647 (red). They were then imaged, live, with differential interference contrast and confocal fluorescence. (A-B) Representative wide and enlarged views of a field of HUVECs with low levels of factor Va and Xa binding. Thin cellular projections did not have visible staining (arrow). (C-D) Representative wide and enlarged views of a field of HUVECs containing colocalized factors Va and Xa on filaments and filopodialike structures at the cell periphery. (E-F). Representative wide and enlarged views of a field of HUVECs showing colocalized binding of factor Va and Xa on punctate structures of the cell body. (G) HUVECs were cultured in 96-well plates in the presence of TNF-α. Prothrombinase activity was measured in a discontinuous assay with a chromogenic thrombin substrate. Prothrombinase activity was inhibited to a greater degree by lactadherin compared with annexin A5. Data are mean ± standard deviation for 2 experiments, each performed in triplicate.

prothrombinase to the highly convex filopodia. We noted a comparable disparity between lactadherin and annexin A5 inhibition of the prothrombinase complex on platelets and leukemia cells.[1,3,8]

Quiescent endothelia have anticoagulant surfaces that prevent clot formation in flowing blood.[31-33,78] In response to various stresses and stimuli the endothelia undergo changes that increase the prothrombotic character.[35,36] These include deencryption of tissue factor,[79] limited and reversible cell exposure of PS,[36,44-47] and transient topological rearrangements of their intercellular junctions.[37-43,80] Elevated cytosolic calcium leads to exposure of membrane PS through TMEM16F, a membrane ion channel that allows transmembrane flux of PS,[81,82] a mechanism for global cellular PS exposure. It is not yet known to what extent it mediates localized exposure of PS on membrane patches, filopodia, and retraction fibers. The results of our study underscore the importance of transient, localized PS exposure on these cells, as well as development of marginal filopodia and contractile filaments.

Our experiments shed light on mechanistic details through which perturbed endothelial cells may cause or contribute to disseminated intravascular coagulation. This disorder occurs in response to severe infections as well as trauma.[83] It is characterized by activation and consumption of coagulation proteins and can lead to organ damage when vessels are occluded, and bleeding when coagulation proteins and platelets are consumed. Activation of

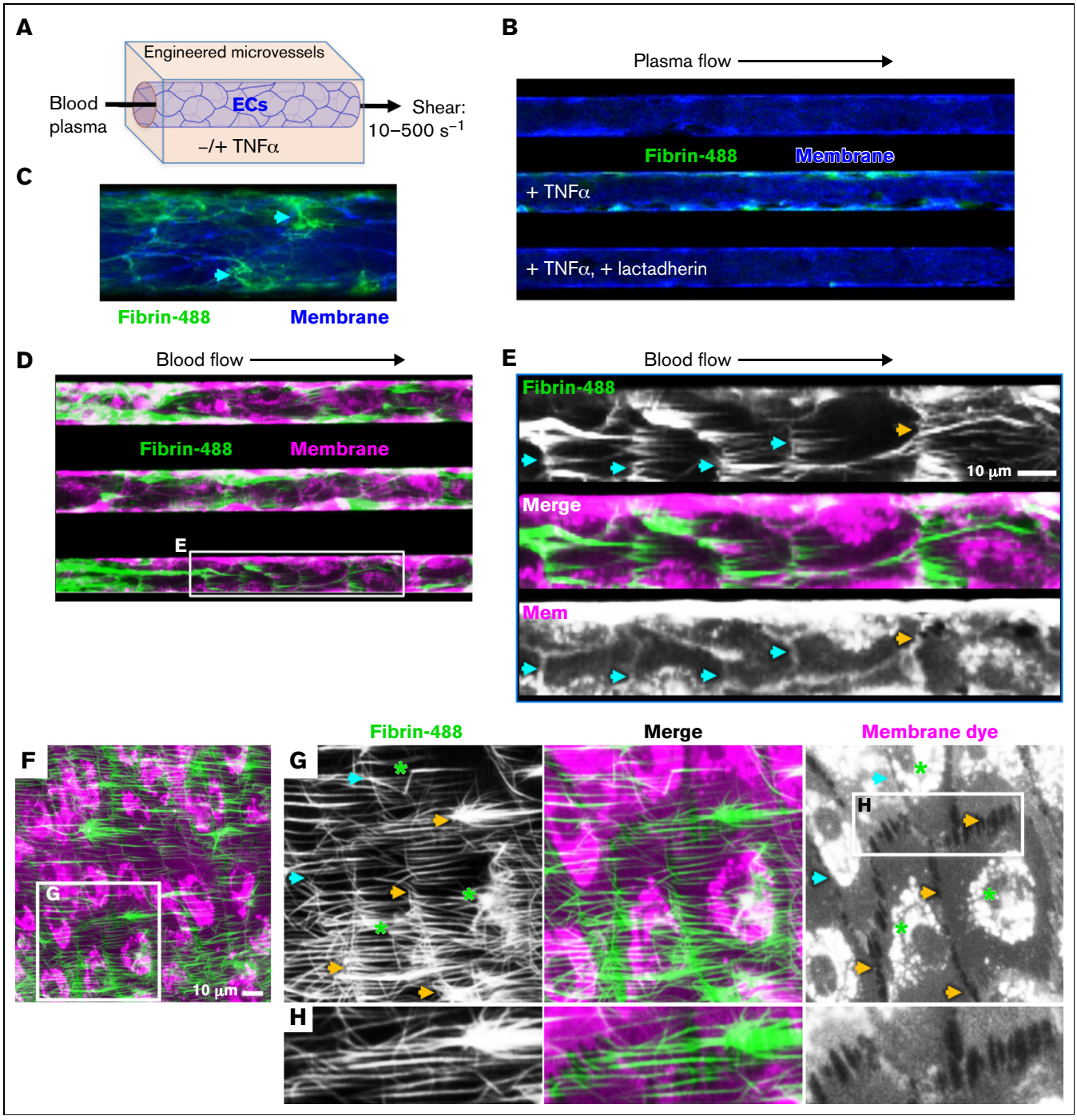

Figure 6. Fibrin deposition around TNF-α–treated endothelial cells under flow conditions. (A) Engineered microvessel setup. HUVECs were grown to confluence on engineered microfluidic substrate and pretreated with TNF-α (100 ng/mL), overnight (B-C) or for 4 hours (D-H). The cell layer was stained with CellMask Orange or Deep Red to visualize the plasma membrane (pseudocolor blue B, C; magenta D-H). Fresh plasma (B, C) was supplemented with corn trypsin inhibitor and fluorescein-labeled fibrinogen (green) and passed through the microfluidic with a sheer of 500 seconds^{-1} for 30 minutes. The microvessels were imaged with fluorescence microscopy. (B) Representative image of fibrin definition in TNF-α–treated microvessel perfused with plasma at 500 seconds^{-1}. Fibrin deposition was not observed in the control channel and was prevented by lactadherin in TNF-α–treated microvessels. (C) Enlarged view of TNF-α–treated microvessel with arrows identifying fibrin deposition at cell junctions or intercellular gaps. (D) Fibrin deposition was also evaluated after perfusion of fresh whole blood, supplemented with corn trypsin inhibitor and fluorescein-fibrinogen at sheer of 100 seconds^{-1}. Fibrin accumulated at cellular junctions (magenta pseudocolor) in a reticular pattern (magenta) as well as in strands in the direction of flow. (E) Enlarged view of boxed region in panel D with fibrin staining shown as white in the top panel, membrane staining as white in the bottom panel, and merged image in the middle. Arrows highlight junctional deposition of fibrin coincident with intact junctions (cyan) or gaps containing junctions with filament-/filopodia-like structures (yellow). (F) Representative field of view under conditions as in panel D, at higher magnification. (G) Enlarged view of boxed region in F with fibrin shown in white (left) membrane in white (right) and merged (middle). Arrows (G-H) highlight junctional deposition of fibrin coincident with intact junctions (cyan) or gaps containing junctions with filament-/filopodia-like structures (yellow). Asterisks indicate occasional fibrin depositions initiated at discrete locations on the cell body. (H) Further enlargement of the boxed region in panel G.

coagulation proteins is triggered, primarily, by tissue factor exposure on endothelial cells and leukocytes in response to TNF-α and cytokines. Recent studies have made it clear that the extent of endothelial activation and injury correlates to clinical outcomes.[84] Notably, a very recent report indicates that a viral gene of SARS-CoV-2, expressed in endothelial cells, causes infected cells to expose PS-support prothrombinase activity.[85] Our studies suggest that the procoagulant activity initially proceeds in a localized manner on highly convex filopodia and retraction fibers at the borders of activated endothelial cells.

In summary, our results demonstrate that the convex topology, together with limited PS exposure on filopodia and marginal protuberances, leads to localized prothrombinase activity. Localization is mediated by the marked preference of factor Va for convex membranes. The procoagulant activity is localized to the margins of, and interspace between, stressed endothelial cells, so that fibrin deposition occurs at the cell margins. These findings are relevant to compartmentalization of coagulation reactions and may contribute to clinical illness in disseminated intravascular coagulation.

Acknowledgments

The authors thank the Harvard Center for Biological Imaging for infrastructure and support.

This work was supported by National Institutes of Health, National Heart, Lung, and Blood Institute grant, R01HL104006 (C.V.C.) and by a Merit Award of the Veterans Administration (G.E.G).

Authorship

Contribution: C.V.C. designed the experiments, analyzed the results, prepared and revised the figures, and drafted the manuscript; D.N.N., Y.S., J.S., and V.A.N. performed the experiments, analyzed the results, and prepared the figures; J.T.R. reviewed the results, prepared the critical reagent; W.L. designed the research, analyzed the results, and reviewed the manuscript; and G.E.G. conceived the project, designed the research, analyzed the results, and revised the manuscript.

Conflict-of-interest disclosure: The authors declare no competing financial interests.

ORCID profiles: Y.S., 0000-0002-7509-9266; V.A.N., 0000-0002-9846-0907; J.T.R., 0000-0002-2809-7225; W.A.L., 0000-0002-0325-7990; G.E.G., 0000-0002-9582-2204.

Correspondence: Gary E. Gilbert, VA Boston Healthcare Center, 1400 VFW Pkwy, West Roxbury, MA 02132; email: gary_gilbert@hms.harvard.edu and gary.e.gilbert.md@gmail.com.

References

1. Shi J, Shi Y, Waehrens LN, Rasmussen JT, Heegaard CW, Gilbert GE. Lactadherin detects early phosphatidylserine exposure on immortalized leukemia cells undergoing programmed cell death. *Cytometry A*. 2006;69A(12):1193-1201.
2. Waehrens LN, Heegaard CW, Gilbert GE, Rasmussen JT. Bovine lactadherin as a calcium-independent imaging agent of phosphatidylserine expressed on the surface of apoptotic HeLa cells. *J Histochem Cytochem*. 2009;57(10):907-914.
3. Zhou J, Shi J, Hou J, et al. Phosphatidylserine exposure and procoagulant activity in acute promyelocytic leukemia. *J Thromb Haemost*. 2010;8(4):773-782.
4. Sakurai Y, Hardy ET, Ahn B, et al. A microengineered vascularized bleeding model that integrates the principal components of hemostasis. *Nat Commun*. 2018;9(1):509.
5. van den Eijnde SM, van den Hoff MJ, Reutelingsperger CP, et al. Transient expression of phosphatidylserine at cell-cell contact areas is required for myotube formation. *J Cell Sci*. 2001;114(Pt 20):3631-3642.
6. Hammill AK, Uhr JW, Scheuermann RH. Annexin V staining due to loss of membrane asymmetry can be reversible and precede commitment to apoptotic death. *Exp Cell Res*. 1999;251(1):16-21.
7. Suzuki J, Umeda M, Sims PJ, Nagata S. Calcium-dependent phospholipid scrambling by TMEM16F. *Nature*. 2010;468(7325):834-838.
8. Shi J, Pipe SW, Rasmussen JT, Heegaard CW, Gilbert GE. Lactadherin blocks thrombosis and hemostasis in vivo: correlation with platelet phosphatidylserine exposure. *J Thromb Haemost*. 2008;6(7):1167-1174.
9. Munnix IC, Strehl A, Kuijpers MJ, et al. The glycoprotein VI-phospholipase Cgamma2 signaling pathway controls thrombus formation induced by collagen and tissue factor in vitro and in vivo. *Arterioscler Thromb Vasc Biol*. 2005;25(12):2673-2678.
10. Zhou J, Zheng Y, Shi J, et al. Daunorubicin induces procoagulant response through phosphatidylserine exposure in red blood cells. *Thromb Res*. 2010;125(2):178-183.
11. Xie R, Gao C, Li W, et al. Phagocytosis by macrophages and endothelial cells inhibits procoagulant and fibrinolytic activity of acute promyelocytic leukemia cells. *Blood*. 2012;119(10):2325-2334.
12. Zhou J, Liu S, Ma M, et al. Procoagulant activity and phosphatidylserine of amniotic fluid cells. *Thromb Haemost*. 2009;101(5):845-851.
13. Shi J, Gilbert GE. Lactadherin inhibits enzyme complexes of blood coagulation by competing for phospholipid-binding sites. *Blood*. 2003;101(7):2628-2636.
14. Dasgupta SK, Guchhait P, Thiagarajan P. Lactadherin binding and phosphatidylserine expression on cell surface-comparison with annexin A5. *Transl Res*. 2006;148(1):19-25.
15. Shi J, Heegaard CW, Rasmussen JT, Gilbert GE. Lactadherin binds selectively to membranes containing phosphatidyl-L-serine and increased curvature. *Biochim Biophys Acta*. 2004;1667(1):82-90.

16. Otzen DE, Blans K, Wang H, Gilbert GE, Rasmussen JT. Lactadherin binds to phosphatidylserine-containing vesicles in a two-step mechanism sensitive to vesicle size and composition. *Biochim Biophys Acta*. 2012;1818(4):1019-1027.

17. Koopman G, Reutelingsperger CP, Kuijten GA, Keehnen RM, Pals ST, van Oers MH. Annexin V for flow cytometric detection of phosphatidylserine expression on B cells undergoing apoptosis. *Blood*. 1994;84(5):1415-1420.

18. Reutelingsperger CPM, Hornstra G, Hemker HC. Isolation and partial purification of a novel anticoagulant from arteries of human umbilical cord. *Eur J Biochem*. 1985;151(3):625-629.

19. Meers P, Daleke D, Hong K, Papahadjopoulos D. Interactions of annexins with membrane phospholipids. *Biochemistry*. 1991;30(11):2903-2908.

20. Meers P, Mealy T. Relationship between annexin V tryptophan exposure, calcium, and phospholipid binding. *Biochemistry*. 1993;32(20):5411-5418.

21. Tait JF, Gibson D. Phospholipid binding of annexin V: effects of calcium and membrane phosphatidylserine content. *Arch Biochem Biophys*. 1992;298(1):187-191.

22. Andree HA, Stuart MC, Hermens WT, et al. Clustering of lipid-bound annexin V may explain its anticoagulant effect. *J Biol Chem*. 1992;267(25):17907-17912.

23. Kenis H, van Genderen H, Bennaghmouch A, et al. Cell surface-expressed phosphatidylserine and annexin A5 open a novel portal of cell entry. *J Biol Chem*. 2004;279(50):52623-52629.

24. Church WR, Jernigan RL, Toole J, et al. Coagulation factors V and VIII and ceruloplasmin constitute a family of structurally related proteins. *Proc Natl Acad Sci USA*. 1984;81(22):6934-6937.

25. Mann KG, Nesheim ME, Church WR, Haley P, Krishnaswamy S. Surface-dependent reactions of the vitamin K-dependent enzyme complexes. *Blood*. 1990;76(1):1-16.

26. Stubbs JD, Lekutis C, Singer KL, et al. cDNA cloning of a mouse mammary epithelial cell surface protein reveals the existence of epidermal growth factor-like domains linked to factor VIII-like sequences. *Proc Natl Acad Sci USA*. 1990;87(21):8417-8421.

27. Macedo-Ribeiro S, Bode W, Huber R, et al. Crystal structures of the membrane-binding C2 domain of human coagulation factor V. *Nature*. 1999;402(6760):434-439.

28. Shao C, Novakovic VA, Head JF, Seaton BA, Gilbert GE. Crystal structure of lactadherin C2 domain at 1.7A resolution with mutational and computational analyses of its membrane-binding motif. *J Biol Chem*. 2008;283(11):7230-7241.

29. Comfurius P, Smeets EF, Willems GM, Bevers EM, Zwaal RFA. Assembly of the prothrombinase complex on lipid vesicles depends on the stereochemical configuration of the polar headgroup of phosphatidylserine. *Biochemistry*. 1994;33(34):10319-10324.

30. Abbott AJ, Nelsestuen GL. Association of a protein with membrane vesicles at the collisional limit: studies with blood coagulation factor Va light chain also suggest major differences between small and large unilamellar vesicles. *Biochemistry*. 1987;26(24):7994-8003.

31. Esmon CT. Structure and functions of the endothelial cell protein C receptor. *Crit Care Med*. 2004;32(5 Suppl):S298-S301.

32. Esmon CT, Owen WG. The discovery of thrombomodulin. *J Thromb Haemost*. 2004;2(2):209-213.

33. Mannucci PM, Bauer KA, Gringeri A, et al. No activation of the common pathway of the coagulation cascade after a highly purified factor IX concentrate. *Br J Haematol*. 1991;79(4):606-611.

34. Wood JP, Ellery PE, Maroney SA, Mast AE. Biology of tissue factor pathway inhibitor. *Blood*. 2014;123(19):2934-2943.

35. Nawroth PP, Stern DM. Modulation of endothelial cell hemostatic properties by tumor necrosis factor. *J Exp Med*. 1986;163(3):740-745.

36. Zheng X, Li W, Song Y, et al. Non-hematopoietic EPCR regulates the coagulation and inflammatory responses during endotoxemia. *J Thromb Haemost*. 2007;5(7):1394-1400.

37. Baluk P, Hirata A, Thurston G, et al. Endothelial gaps: time course of formation and closure in inflamed venules of rats. *Am J Physiol*. 1997;272(1 Pt 1):L155-L170.

38. Baluk P, Bolton P, Hirata A, Thurston G, McDonald DM. Endothelial gaps and adherent leukocytes in allergen-induced early- and late-phase plasma leakage in rat airways. *Am J Pathol*. 1998;152(6):1463-1476.

39. Hirata A, Baluk P, Fujiwara T, McDonald DM. Location of focal silver staining at endothelial gaps in inflamed venules examined by scanning electron microscopy. *Am J Physiol*. 1995;269(3 Pt 1):L403-L418.

40. McDonald DM, Thurston G, Baluk P. Endothelial gaps as sites for plasma leakage in inflammation. *Microcirculation*. 1999;6(1):7-22.

41. Thurston G, Baluk P, Hirata A, McDonald DM. Permeability-related changes revealed at endothelial cell borders in inflamed venules by lectin binding. *Am J Physiol*. 1996;271(6 Pt 2):H2547-H2562.

42. Wojciak-Stothard B, Ridley AJ. Rho GTPases and the regulation of endothelial permeability. *Vascul Pharmacol*. 2002;39(4-5):187-199.

43. McKenzie JA, Ridley AJ. Roles of Rho/ROCK and MLCK in TNF-alpha-induced changes in endothelial morphology and permeability. *J Cell Physiol*. 2007;213(1):221-228.

44. Gao C, Xie R, Yu C, et al. Thrombotic role of blood and endothelial cells in uremia through phosphatidylserine exposure and microparticle release. *PLoS One*. 2015;10(11):e0142835.

45. Zhang Y, Meng H, Ma R, et al. Circulating microparticles, blood cells, and endothelium induce procoagulant activity in sepsis through phosphatidylserine exposure. *Shock*. 2016;45(3):299-307.

46. Slone EA, Pope MR, Fleming SD. Phospholipid scramblase 1 is required for β2-glycoprotein I binding in hypoxia and reoxygenation-induced endothelial inflammation. *J Leukoc Biol*. 2015;98(5):791-804.
47. Sadjadi J, Strumwasser AM, Victorino GP. Endothelial cell dysfunction during anoxia-reoxygenation is associated with a decrease in adenosine triphosphate levels, rearrangement in lipid bilayer phosphatidylserine asymmetry, and an increase in endothelial cell permeability. *J Trauma Acute Care Surg*. 2019;87(6):1247-1252.
48. Popescu NI, Lupu C, Lupu F. Extracellular protein disulfide isomerase regulates coagulation on endothelial cells through modulation of phosphatidylserine exposure. *Blood*. 2010;116(6):993-1001.
49. Hackeng TM, van 't Veer C, Meijers JC, Bouma BN. Human protein S inhibits prothrombinase complex activity on endothelial cells and platelets via direct interactions with factors Va and Xa. *J Biol Chem*. 1994;269(33):21051-21058.
50. Bayerl TM, Bloom M. Physical properties of single phospholipid bilayers adsorbed to micro glass beads: a new vesicular model system studied by 2H-nuclear magnetic resonance. *Biophys J*. 1990;58(2):357-362.
51. Roiter Y, Ornatska M, Rammohan AR, Balakrishnan J, Heine DR, Minko S. Interaction of nanoparticles with lipid membrane. *Nano Lett*. 2008;8(3):941-944.
52. Roiter Y, Ornatska M, Rammohan AR, Balakrishnan J, Heine DR, Minko S. Interaction of lipid membrane with nanostructured surfaces. *Langmuir*. 2009;25(11):6287-6299.
53. Huang C, Mason JT. Geometric packing constraints in egg phosphatidylcholine vesicles. *Proc Natl Acad Sci USA*. 1978;75(1):308-310.
54. Hui KY, Haber E, Matsueda GR. Monoclonal antibodies of predetermined specificity for fibrin: a rational approach to monoclonal antibody production. *Hybridoma*. 1986;5(3):215-222.
55. Tsai M, Kita A, Leach J, et al. In vitro modeling of the microvascular occlusion and thrombosis that occur in hematologic diseases using microfluidic technology. *J Clin Invest*. 2012;122(1):408-418.
56. Brian AA, McConnell HM. Allogeneic stimulation of cytotoxic T cells by supported planar membranes. *Proc Natl Acad Sci USA*. 1984;81(19):6159-6163.
57. Swairjo MA, Concha NO, Kaetzel MA, Dedman JR, Seaton BA. Ca(2+)-bridging mechanism and phospholipid head group recognition in the membrane-binding protein annexin V. *Nat Struct Biol*. 1995;2(11):968-974.
58. Concha NO, Head JF, Kaetzel MA, Dedman JR, Seaton BA. Annexin V forms calcium-dependent trimeric units on phospholipid vesicles. *FEBS Lett*. 1992;314(2):159-162.
59. Meers P, Mealy T. Calcium-dependent annexin V binding to phospholipids: stoichiometry, specificity, and the role of negative charge. *Biochemistry*. 1993;32(43):11711-11721.
60. Pober JS, Lapierre LA, Stolpen AH, et al. Activation of cultured human endothelial cells by recombinant lymphotoxin: comparison with tumor necrosis factor and interleukin 1 species. *J Immunol*. 1987;138(10):3319-3324.
61. Hui KY, Haber E, Matsueda GR. Monoclonal antibodies to a synthetic fibrin-like peptide bind to human fibrin but not fibrinogen. *Science*. 1983;222(4628):1129-1132.
62. Andree HA, Reutelingsperger CP, Hauptmann R, Hemker HC, Hermens WT, Willems GM. Binding of vascular anticoagulant alpha (VAC alpha) to planar phospholipid bilayers. *J Biol Chem*. 1990;265(9):4923-4928.
63. Stern DM, Kaiser E, Nawroth PP. Regulation of the coagulation system by vascular endothelial cells. *Haemostasis*. 1988;18(4-6):202-214.
64. Tracy PB. Regulation of thrombin generation at cell surfaces. *Semin Thromb Hemost*. 1988;14(3):227-233.
65. Ivanciu L, Krishnaswamy S, Camire RM. New insights into the spatiotemporal localization of prothrombinase in vivo. *Blood*. 2014;124(11):1705-1714.
66. Tijburg PN, van Heerde WL, Leenhouts HM, Hessing M, Bouma BN, de Groot PG. Formation of meizothrombin as intermediate in factor Xa-catalyzed prothrombin activation on endothelial cells. The influence of thrombin on the reaction mechanism. *J Biol Chem*. 1991;266(6):4017-4022.
67. Falati S, Gross P, Merrill-Skoloff G, Furie BC, Furie B. Real-time in vivo imaging of platelets, tissue factor and fibrin during arterial thrombus formation in the mouse. *Nat Med*. 2002;8(10):1175-1181.
68. Vandendries ER, Hamilton JR, Coughlin SR, Furie B, Furie BC. Par4 is required for platelet thrombus propagation but not fibrin generation in a mouse model of thrombosis. *Proc Natl Acad Sci USA*. 2007;104(1):288-292.
69. Kroh HK, Panizzi P, Tchaikovski S, et al. Active site-labeled prothrombin inhibits prothrombinase in vitro and thrombosis in vivo. *J Biol Chem*. 2011;286(26):23345-23356.
70. Antonny B. Mechanisms of membrane curvature sensing. *Annu Rev Biochem*. 2011;80(1):101-123.
71. McMahon HT, Boucrot E. Membrane curvature at a glance. *J Cell Sci*. 2015;128(6):1065-1070.
72. Ward KE, Ropa JP, Adu-Gyamfi E, Stahelin RV. C2 domain membrane penetration by group IVA cytosolic phospholipase A_2 induces membrane curvature changes. *J Lipid Res*. 2012;53(12):2656-2666.
73. Ho C, Slater SJ, Stagliano B, Stubbs CD. The C1 domain of protein kinase C as a lipid bilayer surface sensing module. *Biochemistry*. 2001;40(34):10334-10341.
74. Cantor RS. Lipid composition and the lateral pressure profile in bilayers. *Biophys J*. 1999;76(5):2625-2639.
75. Kim SW, Quinn-Allen MA, Camp JT, et al. Identification of functionally important amino acid residues within the C2-domain of human factor V using alanine-scanning mutagenesis. *Biochemistry*. 2000;39(8):1951-1958.

76. Majumder R, Liang X, Quinn-Allen MA, Kane WH, Lentz BR. Modulation of prothrombinase assembly and activity by phosphatidylethanolamine. *J Biol Chem*. 2011;286(41):35535-35542.

77. Medfisch SM, Muehl EM, Morrissey JH, Bailey RC. Phosphatidylethanolamine-phosphatidylserine binding synergy of seven coagulation factors revealed using Nanodisc arrays on silicon photonic sensors. *Sci Rep*. 2020;10(1):17407.

78. Broze GJ Jr, Girard TJ. Tissue factor pathway inhibitor: structure-function. *Front Biosci*. 2012;17(1):262-280.

79. Vatsyayan R, Kothari H, Pendurthi UR, Rao LV. 4-Hydroxy-2-nonenal enhances tissue factor activity in human monocytic cells via p38 mitogen-activated protein kinase activation-dependent phosphatidylserine exposure. *Arterioscler Thromb Vasc Biol*. 2013;33(7):1601-1611.

80. Friedl J, Puhlmann M, Bartlett DL, et al. Induction of permeability across endothelial cell monolayers by tumor necrosis factor (TNF) occurs via a tissue factor-dependent mechanism: relationship between the procoagulant and permeability effects of TNF. *Blood*. 2002;100(4):1334-1339.

81. Hanayama R, Tanaka M, Miwa K, Shinohara A, Iwamatsu A, Nagata S. Identification of a factor that links apoptotic cells to phagocytes. *Nature*. 2002;417(6885):182-187.

82. Yang X, Cheng X, Tang Y, et al. Bacterial endotoxin activates the coagulation cascade through gasdermin D-dependent phosphatidylserine exposure. *Immunity*. 2019;51(6):983-996.e6.

83. Gando S, Levi M, Toh CH. Disseminated intravascular coagulation. *Nat Rev Dis Primers*. 2016;2(1):16037.

84. Walborn A, Rondina M, Mosier M, Fareed J, Hoppensteadt D. Endothelial dysfunction is associated with mortality and severity of coagulopathy in patients with sepsis and disseminated intravascular coagulation. *Clin Appl Thromb Hemost*. 2019;25:1076029619852163.

85. Jacob G, Ludington M, Shabbir A, et al. SARS-CoV-2 ion channel ORF3a enables TMEM16F-dependent phosphatidylserine externalization to augment procoagulant activity of the tenase and prothrombinase complexes [abstract]. *Blood*. 2021;138(21). Abstract 1.